Network pharmacology and in vitro exploration of the antiglioma mechanism of anthocyanins from Lycium ruthenicum Murr
SCI论文
《GENE》中科院三区
2026年6月发表
第一作者



检 索 证 明

经检索《Science Citation Index Expanded》（SCI-EXPANDED）数据库、《Journal Citation Reports》（JCR）数据库和《中国科学院文献情报中心期刊分区表升级版》，以下 1 篇文献的收录简要信息、期刊的影响因子及分区如下：

标题: Network pharmacology and in vitro exploration of the antiglioma mechanism of anthocyanins from Lycium ruthenicum Murr

作者: Zhou, HW (Zhou, Hongwei);Sima, J (Sima, Jinwen);Wang, SL (Wang, Shenglei);Lu, SJ (Lu, Shijia);Liang, JL (Liang, Jialin);Li, XY (Li, Xinyao);Lian, TT (Lian, Tiantian);Wang, CC (Wang, Congcong)

来源出版物: GENE　卷:1008　DOI:10.1016/j.gene.2026.150277　出版时间:NOV 5 2026　提前访问日期:JUN 2026

Web of Science 核心合集中的“被引频次”：0 次

期刊《GENE》2025 年影响因子为 2.7。

经检索《中国科学院文献情报中心期刊分区表升级版》，2025 年分区如下：

刊名	GENE		
年份	2025		
ISSN/EISSN	0378-1119/1879-0038		
Review	否		
OA Journal Index（OAJ）	否		
Open Access	否		
Web of Science	SCIE		
	学科	分区	Top 期刊
小类	GENETICS & HEREDITY 遗传学	3	
大类	生物学	3	否

特此证明

（详细内容见附件）

扫描二维码查看报告

郑州大学图书馆

教育部科技查新工作站 Z12

检索人：张逸迪

2026 年 09 月 03 日

注：因 JCR 数据更新滞后，新出版论文的期刊影响因子以最新版 JCR 数据为参考。

第 1 条，共 1 条

标题: Network pharmacology and in vitro exploration of the antiglioma mechanism of anthocyanins from Lycium ruthenicum Murr

作者: Zhou, HW (Zhou, Hongwei);Sima, J (Sima, Jinwen);Wang, SL (Wang, Shenglei);Lu, SJ (Lu, Shijia);Liang, JL (Liang, Jialin);Li, XY (Li, Xinyao);Lian, TT (Lian, Tiantian);Wang, CC (Wang, Congcong)

来源出版物: GENE **卷:** 1008 **DOI:** 10.1016/j.gene.2026.150277 **出版年:** NOV 5 2026 **提前访问日期**:JUN 2026

Web of Science 核心合集中的 "被引频次": 0

被引频次合计: 0

使用次数 (最近 180 天): 4

使用次数 (2013 年至今): 4

引用的参考文献数: 55

摘要: Background: Lycium ruthenicum Murr (black goji berry) is a traditional edible ethnomedicine in Northwest China, valued for metabolic regulation. Building on the ethnopharmacological background of L. ruthenicum, the research employed network pharmacology, in vitro assays, and molecular docking to explore the inhibitory effects of L. ruthenicum anthocyanins (LRA) on human glioma cells and to elucidate their potential molecular mechanisms. Methods: The active components and targets of LRA were identified using network pharmacology. Molecular docking experiments and U251 cell experiments were conducted to determine how LRA affects proliferation, migration, apoptosis, cell cycle progression, and reactive oxygen species formation. Results: welve key LRA components and 66 glioma-related targets were identified. Enrichment analysis suggests LRA's antiglioma effects may involve apoptosis, cell migration, the PI3K-AKT and MAPK pathways. In vitro, LRA inhibited U251 cell growth and migration, caused G2/M-phase arrest, and increased reactive oxygen species. It reduced Bcl-2 levels while raising Bax, P53, Caspase-3, and Caspase-9. Conclusion: LRA may combat glioma by inhibiting the PI3K-AKT signaling trajectory, altering the Bax/Bcl-2 ratio, boosting Caspase activity, inducing G2/M arrest, and inhibiting proliferation and migration.

入藏号: WOS:001806951900001

PubMed ID: 42314778

语言: English

文献类型: Article

作者关键词: Lycium ruthenicum;Anthocyanin;Human glioma;U251 cells;Network pharmacology;In vitro experiments

KeyWords Plus: APOPTOSIS

地址: [Zhou, Hongwei; Wang, Shenglei; Lu, Shijia; Lian, Tiantian] North Henan Med Univ, Coll Life Sci & Technol, Xinxiang 453003, Peoples R China;[Sima, Jinwen] North Henan Med Univ, Coll Clin Med, Xinxiang 453003, Peoples R China;[Liang, Jialin] Qinghai Univ, Coll Ecol Environm Engn, Xining 810016, Peoples R China;[Li, Xinyao] North Henan Med Univ, Coll Nursing, Xinxiang 453003, Peoples R China;[Wang, Congcong] Suzhou Suncadia Biopharmaceut Co Ltd, Suzhou 2150000, Peoples R China

通讯作者地址: [Sima, Jinwen] (corresponding author), North Henan Med Univ, Coll Clin Med, Xinxiang 453003, Peoples R China

电子邮件地址: 17532053@nhmu.edu.cn;simajinwen@126.com

出版商:ELSEVIER

出版商地址: RADARWEG 29, 1043 NX AMSTERDAM, NETHERLANDS

Web of Science Index : 《Science Citation Index Expanded》（SCI-EXPANDED）

Web of Science 类别: Genetics & Heredity

研究方向: Genetics & Heredity

IDS 号:KH3EG

ISSN: 0378-1119

eISSN: 1879-0038

来源出版物页码计数: 13

基金资助致谢: This research was funded by the National Natural Science Founda-tion of China, grant number 82072802; the Backbone Teachers Program of North Henan Medical University, grant number SQ2023GGJS03; Key Scientific Research Project of Institutions of Higher Education in Henan Province, grant number 25A310027 and the Henan Provincial Innova-tion and Entrepreneurship Training Program (Grant No. S202513505014) .

基金资助机构	授权号
National Natural Science Founda-tion of China	82072802
Backbone Teachers Program of North Henan Medical University	SQ2023GGJS03
Key Scientific Research Project of Institutions of Higher Education in Henan Province	25A310027
Henan Provincial Innova-tion and Entrepreneurship Training Program	S202513505014

ESI 高被引论文: N

ESI 热点论文: N

输出日期: 2026 年 09 月 03 日

Gene 1008 (2026) 150277

Contents lists available at ScienceDirect

Gene

journal homepage: www.elsevier.com/locate/gene

Network pharmacology and *in vitro* exploration of the antiglioma mechanism of anthocyanins from *Lycium ruthenicum* Murr

Hongwei Zhou [a], Jinwen Sima [b,*], Shenglei Wang [a], Shijia Lu [a], Jialin Liang [c], Xinyao Li [d], Tiantian Lian [a], Congcong Wang [e]

[a] *Collgege of Life Sciences and Technologies, North Henan Medical University, Xinxiang 453003, China*
[b] *College of Clinical Medicine, North Henan Medical University, Xinxiang 453003, China*
[c] *College of Ecological and Environmental Engineering, Qinghai University, Xining 810016, China*
[d] *College of Nursing, North Henan Medical University, Xinxiang 453003, China*
[e] *Suzhou Suncadia Biopharmaceuticals Co., Ltd, Suzhou 2150000, China*

ARTICLE INFO

Keywords:
Lycium ruthenicum
Anthocyanin
Human glioma
U251 cells
Network pharmacology
In vitro experiments

ABSTRACT

Background: Lycium ruthenicum Murr (black goji berry) is a traditional edible ethnomedicine in Northwest China, valued for metabolic regulation. Building on the ethnopharmacological background of *L. ruthenicum*, the research employed network pharmacology, in vitro assays, and molecular docking to explore the inhibitory effects of *L. ruthenicum* anthocyanins (LRA) on human glioma cells and to elucidate their potential molecular mechanisms.

Methods: The active components and targets of LRA were identified using network pharmacology. Molecular docking experiments and U251 cell experiments were conducted to determine how LRA affects proliferation, migration, apoptosis, cell cycle progression, and reactive oxygen species formation.

Results: welve key LRA components and 66 glioma-related targets were identified. Enrichment analysis suggests LRA's antiglioma effects may involve apoptosis, cell migration, and PI3K–AKT and MAPK pathways. In vitro, LRA inhibited U251 cell growth and migration, caused G2/M−phase arrest, and increased reactive oxygen species. It reduced Bcl-2 levels while raising Bax, P53, Caspase-3, and Caspase-9.

Conclusion: LRA may combat glioma by inhibiting the PI3K–AKT signaling trajectory, altering the Bax/Bcl-2 ratio, boosting Caspase activity, inducing G2/M arrest, and inhibiting proliferation and migration.

1. Introduction

Glioblastoma (GBM), main intracranial malignancy, constitutes roughly 30% of all tumors in the central nervous system (CNS), then constitutes 81% of malignant tumors in the brain (Fakhoury et al., 2021). Its notable characteristics—high morbidity, frequent recurrence, and dismal prognosis—have made it a major focus of clinical and scientific research (Ghouzlani et al., 2021). In China, the annual incidence of GBM ranges from 5 to 8 cases per 100,000 individuals (Gao et al., 2023), with 3- and 5-year postoperative survival rates of 40.63% and 17.19%, respectively (Liu et al., 2018). Despite advances in therapeutic approaches, treatment efficacy remains severely limited by limited drug penetration efficiency through the blood–brain barrier and inherent tumor heterogeneity. Furthermore, nearly all GBM patients eventually experience recurrence, and the prognosis after relapse is significantly worse (Arrieta et al., 2024). Therefore, the identification of novel anti-GBM bioactive compounds with safe natural origins and well-defined molecular targets has become an urgent priority in both clinical practice and scientific research.

Currently, natural products reflect escalating prominence as sources of novel antitumor agents, owing to their abundance, favorable safety profiles (low toxicity and minimal side effects), and promising anti-neoplastic potential (Erkisa et al., 2022). The thorny shrub of the genus Lycium (family Solanaceae), L. *ruthenicum* Murr., is endemic to arid and saline-alkaline habitats situated in the China (Northwest) including the Qinghai-Tibet Plateau. The mature fruits of dark purple-black coloration, commonly referred to as "black goji berries," are distinguished by their substantial concentration of bioactive anthocyanins. These compounds have been proven to exhibitsignificant cancer-inhibiting, antioxidant, and neuroprotective properties (Liang et al., 2025). Traditional

* Corresponding author.
E-mail addresses: 17532053@nhmu.edu.cn (H. Zhou), simajinwen@126.com (J. Sima).

https://doi.org/10.1016/j.gene.2026.150277
Received 27 February 2026; Received in revised form 1 June 2026; Accepted 18 June 2026
Available online 18 June 2026
0378-1119/© 2026 Elsevier B.V. All rights are reserved, including those for text and data mining, AI training, and similar technologies.

Tibetan medical classic *The Four Medical Tantras (rgyud bzhi)* documents its efficacy in regulating systemic balance and alleviating inflammation, while the *Uyghur Pharmacopoeia* describes its role in nourishing the brain and maintaining physiological homeostasis—effects that are corroborated by contemporary pharmacological investigations demonstrating the medicinal materials' neuroprotective potential against oxidative stress and neurodegenerative conditions (Li et al., 2024). Given these ethnomedicinal and preclinical evidence, coupled with the pressing demand for novel therapeutics against GBM, which is a highly aggressive neurological malignancy, this study focuses on *L. ruthenicum* anthocyanins (LRAs) to investigate their anti-GBM potential and the underlying molecular mechanisms.

Anthocyanins, also known as anthocyanidins, are principal bioactive flavonoids prevalent in L. ruthenicum and have been documented to demonstrate various pharmacological characteristics, including anti-inflammatory and anticancer, cardioprotective, and metabolic regulatory effects. Plant-derived polyphenols have been identified as promising candidates in anticancer study, primarily due to their ability to trigger tumor cell apoptosis and inhibit cell migration and invasion—mechanisms that have been validated in multiple preclinical studies (Hu et al., 2025; Xie et al., 2023; Zeng et al., 2024). For instance, Fan et al. (Fan et al., 2022) revealed that *L. ruthenicum* anthocyanins (LRAs) significantly decreased the viability and clonogenic survival of HepG-2 hepatocellular carcinoma cells through instrigating G_2/M stage arrest and apoptosis. In a similar vein, Li et al. (Li et al., 2021) demonstrated that LRAs suppressed propagation and resulted apoptosis in DU-145 prostate cancer cells by activating ROS/PTEN/PI3K/Akt/Caspase-3 activating pathway. Even so, inhibitory effects of LRAs on glioma, and their major molecular targets and functional mechanisms, remain inadequately elucidated. Notably, studies integrating traditional ethnomedicinal perspectives with modern pharmacological analysis are scarce, limiting the translational potential of this traditional remedy for glioma therapy.

To address this research gap, the current study explored the antiglioma potential of LRAs through a comprehensive approach that integrates network pharmacology, cellular measurements, and molecular docking. Network pharmacology was applied to determine possible antiglioma targets and signaling conduits, and to determine the binding affinities between significant anthocyanin monomers and aimed proteins molecular docking was applied. The effects of LRAs on U251 human GBM cells were assessed usingMTT assay (proliferation), scratch wound healing assay (migration), cell cycle distribution, and ROS concentrations (flow cytometry). To elucidate the regulatory effects on apoptosis-related genes, proteins, and key signaling conduits, Western blotting and Quantitative real-time PCR (qPCR) were conducted. Collectively, these findings provide preclinical evidence supporting *Lycium ruthenicum* Murr. anthocyanins (LRA) as a promising natural-derived adjunctive agent for GBM treatment, highlighting their therapeutic potential in GBM pharmaceutical R&D.

2. Materials and methods

2.1. Components

2.1.1. Drug

The Northwest Institute of Plateau Biology, part of the Chinese Academy of Sciences in Xining, China, provided the LRA (Anthocyanin purity > 85%).

2.1.2. Cell

This investigation made use of a human glioma cell line acquired from the Cell Bank of the Chinese Academy of Sciences in Shanghai, China.

2.1.3. Major reagents and instruments

The principal kits and antibodies were utilized in this research were as follows: MTT Cell Proliferation Assay Kit (Lot No. 804W053, Solarbio Science & Technology Co., Ltd., Beijing, China); Reactive Oxygen Species Assay Kit (Lot No. 36524584ZA, Beijing Lanjieke Technology Co., Ltd.); Reverse Transcription Kit (Lot No. 7E2180H4, Vazyme Biotech Co., Ltd., Nanjing, China); SYBR qPCR Master Mix (Lot No. 7E0350F5, Vazyme Biotech Co., Ltd., Nanjing, China); BCA Protein Concentration Assay Kit (Lot No. Z928240816, Beyotime Biotechnology, Shanghai, China); SDS-PAGE Gel Quick Preparation Kit (Lot No. 20325ES62, Yeasen Biotechnology Co., Ltd.); ECL Chemiluminescence Reagent Kit (Lot No. A063250420, Beyotime Biotechnology, Shanghai, China); labeled goat anti-rabbit antibody (Lot No. SA00001-1, SA22221-2, Wuhan Sanying Biotechnology Co., Ltd., Wuhan, China); and antibodies against apoptosis-related proteins (Bcl-2, Bax, p53, Caspase-3, and Caspase-9) (Lot No. 12789, 50599, 10442, 25128, 10380, Wuhan Sanying Biotechnology Co., Ltd., Wuhan, China).

The major instruments used were as follows: flow cytometer (Beckman Colter Biotechnology Co., Ltd.); Zeiss Observer 7 automated live-cell imaging workstation (Model Axio Observer; Carl Zeiss AG, Germany); Applied Biosystems Observer 7 Automated Live-Cell PCR System (Thermo Fisher Scientific Inc.); and Varioskan LUX multimode microplate reader (Thermo Fisher Scientific Inc.).

2.2. Network pharmacology analysis

2.2.1. Collection of active components from LRAs and prediction of target proteins

Information on the medicinal constituents of black goji berries was not available in mainstream traditional Chinese medicine (e.g., TCMSP, TCMID, ETCM) or natural product databases (e.g., NPASS, SuperNatural II). Therefore, the major active compounds of LRAs were identified through a literature review, and molecular structure files were retrieved from PubChem (Kim et al., 2023). For unrecorded compounds, molecular structures were manually constructed using RDKit 2.0 software (https://decimer.ai/) based on published chemical structures. All obtained molecular structure files (SDF format) were processed using RDKit (Duarte Ramos Matos et al., 2023) to extract and validate standardized isomeric SMILES strings, ensuring accuracy for subsequent analytical inputs.

To ensure comprehensiveness and reliability in predicting the primary active compounds of LRAs and their target proteins, six target prediction databases were utilized: the Swiss Target Prediction repository (http://swisstargetprediction.ch/) (Daina et al., 2019), the Similarity Ensemble Approach (SEA) repository (https://sea.bkslab.org/) (Keiser et al., 2007), the Target Net repository (http://targetnet.scbdd.com/home/index/) (Yao et al., 2016), the SuperPred database (https://prediction.charite.de/) (Gallo et al., 2022), the TTD database (https://db.idrblab.net/ttd/) (Zhou et al., 2024), and the PharmMapper database (https://lilab-ecust.cn/pharmmapper/index.html) (Wang et al., 2017).

2.2.2. GBM disease target prediction

Using "glioma" as the keyword, disease-associated targets were retrieved from four authoritative databases: GeneCards database (https://www.genecards.org/) (Stelzer et al., 2016), MalaCards database (https://www.malacards.org/) (Rappaport et al., 2017), OMIM database (https://www.omim.org/) (Hamosh et al., 2005), and CTD database (https://ctdbase.org/) (Davis et al., 2025).

2.2.3. Prediction of drug-disease intersection targets

Following the processes of collation, deduplication, and statistical analysis of the functional targets of latency-reversing agents (LRAs) and the disease targets associated with glioblastoma multiforme (GBM), the datasets designated as DrugTargets and DiseaseTargets were established. Subsequently, a Venn diagram illustrating the intersecting targets was developed using Venny 2.1, accessible via https://bioinfogp.cnb.csic.es/tools/venny/index.html, thereby identifying potential targets for LRAs within the context of glioma.

2.2.4. Building protein–protein interaction networks

The IntersectionTargets were integrated into the database (STRING) (https://cn.string-db.org/) (Szklarczyk et al., 2023) to facilitate the analysis of interactions among the target proteins. The parameter of the species was designated as "Homo sapiens," and protein interactions with a minimum confidence score of ≥ 0.4 were extracted in TSV format. Subsequently, these numbers were imported into Cytoscape version 3.9.1 (Buzzao et al., 2024) to enable enhanced exploration and the creation of the protein–protein interaction (PPI) network. Core functional targets were identified using the Centiscape 2.2 plugin for Cytoscape, applying betweenness, degree, and closeness centrality algorithms.

2.2.5. Pathway enrichment examination

The GSE119468 dataset was downloaded from the NCBI GEO database (Barrett et al., 2013). An ssGSEA (He et al., 2022) enrichment analysis was performed on the normal cultured U251 cell line, and the leading ten pathways were significantly detected. The central targets selected in the previous part (2.2.4) were submitted to the DAVID database (https://david.ncifcrf.gov/) (Dennis et al., 2003), selecting the species (*Homo sapiens*) for gene ontology (GO) biological overrepresentation assessment and KEGG biochemical route overrepresentation assessment. Results were filtered at $P < 0.01$, with data statistics, analysis, and plotting conducted according to biotic mechanism (BP), cell-based part (CC), molecule-based role (MF), and KEGG routes.

2.2.6. Molecular docking

To investigate the potential binding modes and affinity between the main active monomers in LRA and the core anti-glioma targets screened by network pharmacology, this study employed molecular docking technology for validation. The three-dimensional crystal structures of the core target proteins were downloaded from the RCSB Protein Data Bank (PDB) (https://www.rcsb.org/) (Burley et al., 2023) and saved in the standard PDB format. The obtained protein structures were processed using PyMOL(Rosignoli and Paiardini, 2022), which included removing water molecules, irrelevant ligands, and redundant subunits from the original structures to obtain a clean receptor protein structure for subsequent docking. The two-dimensional chemical structures of the 12 main active monomer components of LRA were determined through literature research, and their three-dimensional structure files (in SDF format) were retrieved from the PubChem database. For compounds not included in the database, their structures were manually constructed using the RDKit toolkit based on published chemical structures. Subsequently, the SDF format files of all active components were uniformly converted into the mol2 format suitable for molecular docking using OpenBabel software (version 3.1.1) (O'Boyle et al., 2011). The molecular docking validation in this study was performed using AutoDock Vina (Buccheri and Rescifina, 2025). Prior to docking, both the receptor protein and the small molecule ligands were preprocessed: relevant tools were used to add hydrogen atoms and assign Gasteiger charges to the protein receptor, and the final structure was saved in pdbqt format; simultaneously, rotatable bonds were defined for the small molecule ligands, which were also saved in pdbqt format. During the docking process, the processed protein structure was defined as the rigid receptor, and the small molecule ligand was defined as the flexible ligand. The dimensions and center coordinates of the docking search space (i.e., the docking box) were set according to the location of the target protein's active pocket to ensure comprehensive coverage of potential binding regions. Key docking parameters (such as exhaustiveness) were set to the software's defaults or optimized based on common research practices to ensure sufficient conformational sampling and reliable results. The program performed multiple independent docking calculations, outputting multiple binding conformations ranked by binding free energy. After docking completion, AutoDock Vina calculated a best binding energy (expressed in kcal/mol) for each receptor-ligand complex. A negative binding energy value indicates that the binding process can occur spontaneously, and a lower value (i.e., a larger negative value) typically indicates stronger binding affinity between the two. The calculated best binding energy data were compiled, and a heatmap was generated for visualization, where the color intensity represents the strength of the binding energy.

*2.3.*Experiments conducted on cells in a controlled environment.

2.2.7. Cell proliferation activity assay (MTT method)

During the logarithmic growth phase, U251 cells were coated at a concentration of 5,000 cells per well in 96-well plates and left overnight to adhere.Lycium ruthenicum Murr. anthocyanins (LRAs) were administered at three concentration gradients (100, 300, and 500 μg/mL), with a blank control group (without LRA treatment) set for comparison. Subsequent to the removal of the medium, 10 μL of MTT was integrated into each well, succeeded by 4hrs incubation duration. The optical density (OD) at a wavelength of 490 nm was measured utilizing a microplate reader. The inhibition rate was computed using the following formula: Inhibition rate (%) = [(OD of the control group − OD of the experimental group)/(OD of the control group − OD of the blank group)] × 100.

2.2.8. Cell migration assay – cell scratch technique

U251 cells at the logarithmic development stage (log-phase) were plated on 6-well plates (500,000 cells/well) and incubated for 24 h. Then, the culture was smashed with a 10 μl sterile pipette tip and rinsed with PBS. LRAs were added at a particular concentrationgradient of 100, 300, and 500 μg/mL, and a control group with no LRA was also included. Cell migration was observed via live-cell imaging at 0, 24, and 48 h after treatment, and images were recorded.

2.2.9. Cell Cycle examination – flow cytometry

In the logarithmic growth stage, U251 cells were added to 6-well culture plates, with each well containing 500,000 cells. The liquid medium was discarded after 24 h of culture. LRAs were added to the culture plates at 100, 300, and 500 μg/mL, and a control group with no LRA was also included. Control and treated cells were digested by trypsin and centrifuged after 24 h. Cells underwent resuspension and another round of centrifugation, followed by discarding the supernatant. Cells were fixed with 70% ethanol, and the fixative was subsequently discarded. Propidium iodide was added to the cells, and the cell cycle was assessed by flow cytometry.

2.2.10. Apoptosis detection – ROS assay

U251 cells in the log phase were inoculated with 5000 cells per well in 96-well plates and protected at 37 °C in 5% CO_2 after 24 hours.

Table 1
Primers for qRT-PCR used in this study.

Gene Name	NCBI Accession Number	Forward Primer Sequence (5'→3')	Reverse Primer Sequence (5'→3')	Primer Position (nucleotide coordinates)	Region(intron/exon)
β-action	NM_001101.5	ATGTTTGAGACCTTCAACAC	CACGTCACACTTCATGATGG	451-470/926-945	exon 4/exon 5
Bax	NM_001291431.2	CCCGAGAGGTCTTTTTCCGAG	CCAGCCCATGATGGTTCTGAT	118-138/252-272	exon 2/exon 3
Caspase-3	NM_004346.4	TTTTTCAGAGGGGATCGTTG	CGGCCTCCACTGGTATTTTA	659-678/790-809	exon 6/exon 7
Bcl-2	NM_000633.3	GCCTTCTTTGAGTTCGGTGGG	GCCGGTTCAGGTACTCAGTCATC	1327-1347/1410-1432	exon 2/exon 2

Latency-reversing agents (LRA) were then added to the discarded medium at 100, 300 and 500 ug/mL. The medium was again incubated after 24 hours and added 90 μL of diluted DCFH-DA solution. The plates were incubated and covered with the dark in 30 minutes. After the medium was removed, fresh DMEM was used to clean the cells and live-cell imaging was performed.

2.2.11. Cell mRNA expression analysis – qRT-PCR

Log-phase U251 cells were seeded into 6-well plates (500,000 cells/well) and incubated for 24 h, after which the liquid phase was removed. LRAs were added at 100, 300, and 500 μg/mL, and a control group with no LRA added was also included. Samples were incubated for a further 24 h. RNA was isolated from cellular samples using Trizol agent. RNAs were converted into cDNAs employing a commercial kit. The qPCR was conducted in a 10 μl volume with thermocycling conditions of an initial 5-minute denaturation (at 95 °C), succeeded by 40 cycles of 95 °C (10 secs) and 55 °C (30 secs). Level of expression for BAX, BCL-2, and CASPASE-3 were evaluated using the 2−ΔΔCt method (Hamed et al., 2022).The primer sequences used in this study are listed in Table 1, along with their detailed information, including NCBI accession numbers, nucleotide positions, and intron/exon boundaries.

2.2.12. Detection of cellular protein expression – western blot

During the logarithmic growth phase, U25 cells were introduced into 6-well plates with 500,000 cells/well and incubated for 24 hours.Subsequently, the culture medium was aspirated. Latency-reversing agents (LRAs) were administered at 100, 300, and 500 μg/mL concentrations, with a control group maintained for comparison. Following a further 24-hour incubation period, cells were harvested from the culture dishes by a cell scraper and relocated into 1.5 mL Eppendorf tubes. The cell suspensions were centrifuged at 12,000 rpm for 9 minutes at 4 °C, and the supernatant was discarded. RIPA lysis buffer augmented with a protease inhibitor cocktail at a 100:1 ratio was added, and the samples were agitated on ice for 30 minutes to promote cell lysis. Protein levels were measured with the BCA assay, then normalized with PBS and 5 × loading buffer, and denatured at 100 °C for 10 minutes.

The following steps were performed for the electrophoresis and membrane transfer: (1) electrophoresis was performed on a 10% SDS-PAGE gel, with 80 Volts as initial point (30 mins), then for another 45 mins, it was raised to 120 V; (2) proteins from gel were blotted onto PVDF membranes at a constant power of 24 W (approximately 100 min), and membranes were blocked with the 3% BSA/ TBST solution at ambient temperature 1 h; (3) main antibody were used to to agitate for 2 h at room temp (a.r.t), and membranes were incubated overnight at 4 °C; (4) the following day, membranes were rinsed 3 times with TBST (5 min each rinse) and finally agitated with the secondary antibody under shaking (ihr at room temp); (5) membranes were washed three times with TBST (8 min per wash); (6) membranes were developed using ECL chemiluminescent reagent under a ChermDoc imaging system; and (7) strength of the band was evaluated with ImageJ software version 1.46 (Cabuk et al., 2021), and target protein expression levels were compared to the internal control.

2.3. Statistical methods

Each experimental group included an experimental triplicate. Results were obtained as average ± standard deviation ($\bar{x}$ ± s) and examined via GraphPad Prism 10.1.2. To analyze the variances among groups, a one-way ANOVA was utilized. Post-hoc analyses were carried out after the ANOVA. Statistical significance for variances was established at $P < 0.05$.

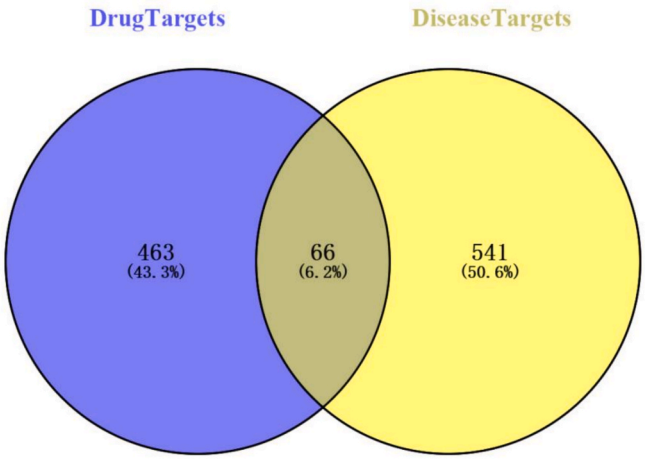

Fig. 1. Venn diagram of LRA and glioma targets.

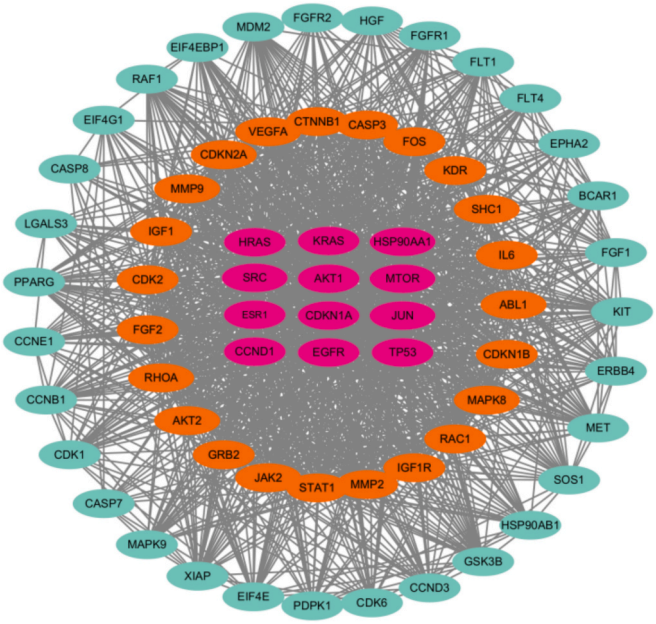

Fig. 2. PPI network analysis of active components of *Lycium ruthenicum Murr.* anthocyanins and glioma.

3. Results and analysis

3.1. Collection of active LRAs and identification of their targets in GBM

Through a literature review, 12 primary active LRAs were identified (Zeng et al., 2024; Wang et al., 2018). Concurrently, RDKit software was used to read the SDF files of these compounds, yielding the corresponding SMILES structural codes of the compounds. The full chemical names and SMILES strings of all 12 components, crucial for network pharmacology analyses (exist in the Supplementary Material Table S1). The action targets of LRAs were predicted using Swiss Target Prediction, SEA, TargetNet, SuperPred, TTD, and PharmMapper platforms, yielding 529 DrugTargets. GBM-associated disorder targets were extracted via GeneCards, MalaCards, OMIM, and the CTD database. After collation, cleaning, and deduplication of the data, 607 DiseaseTargets were obtained. The intersection of those two datasets was determined through Venny 2.1 to draw a Venn diagram demonstrating the overlap between drug and disease targets (Fig. 1).

Analyzing the 66 intersecting targets revealed that LRAs primarily

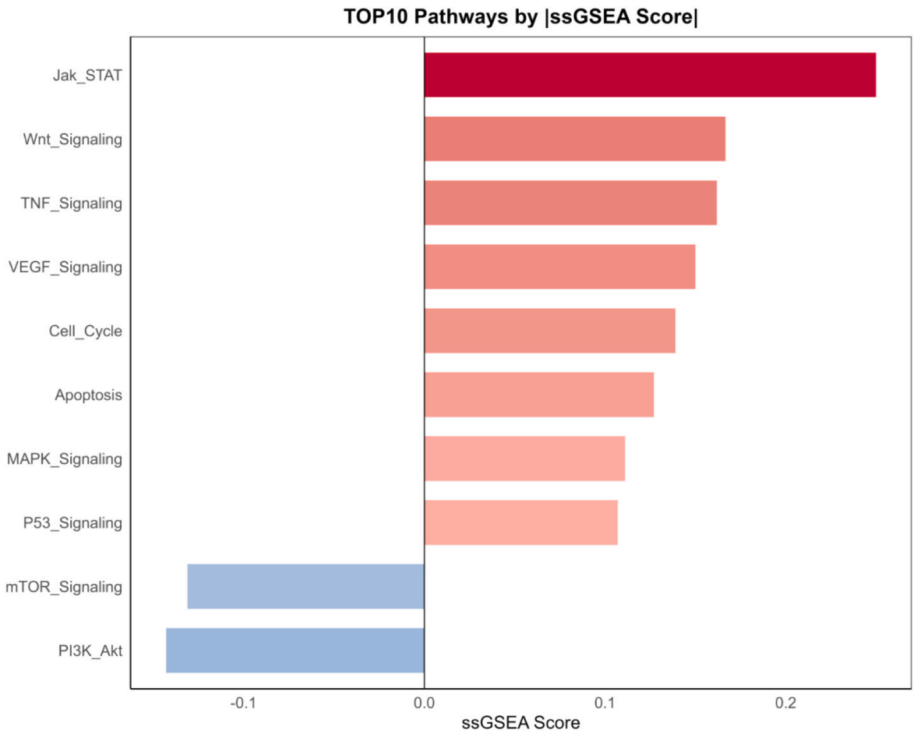

Fig. 3. TOP10 Pathways from ssGSEA Analysis of the U251-MG Cell Line.

act on brain glioma targets involved in signal transduction regulation and core cellular biological processes. These encompass the following categories: protein kinases (e.g., EGFR, AKT), apoptosis and cell cycle regulation-related proteins (e.g., members of the Caspase family, CDKs), epigenetic regulators, molecular chaperones and stress-response proteins, diverse enzymes and metabolism-related proteins, and other functional proteins, such as growth factors and signal transduction adaptor proteins. The distribution characteristics of these targets collectively suggest that LRAs may exert their potential inhibitory effect on glioma through multitarget synergistic action and regulation of multiple pathways.

3.2. *Examination of protein–protein interaction networks*

The LRAs were analyzed by importing the 66 target proteins associated with glioblastoma multiforme (GBM) into the database (STRING)

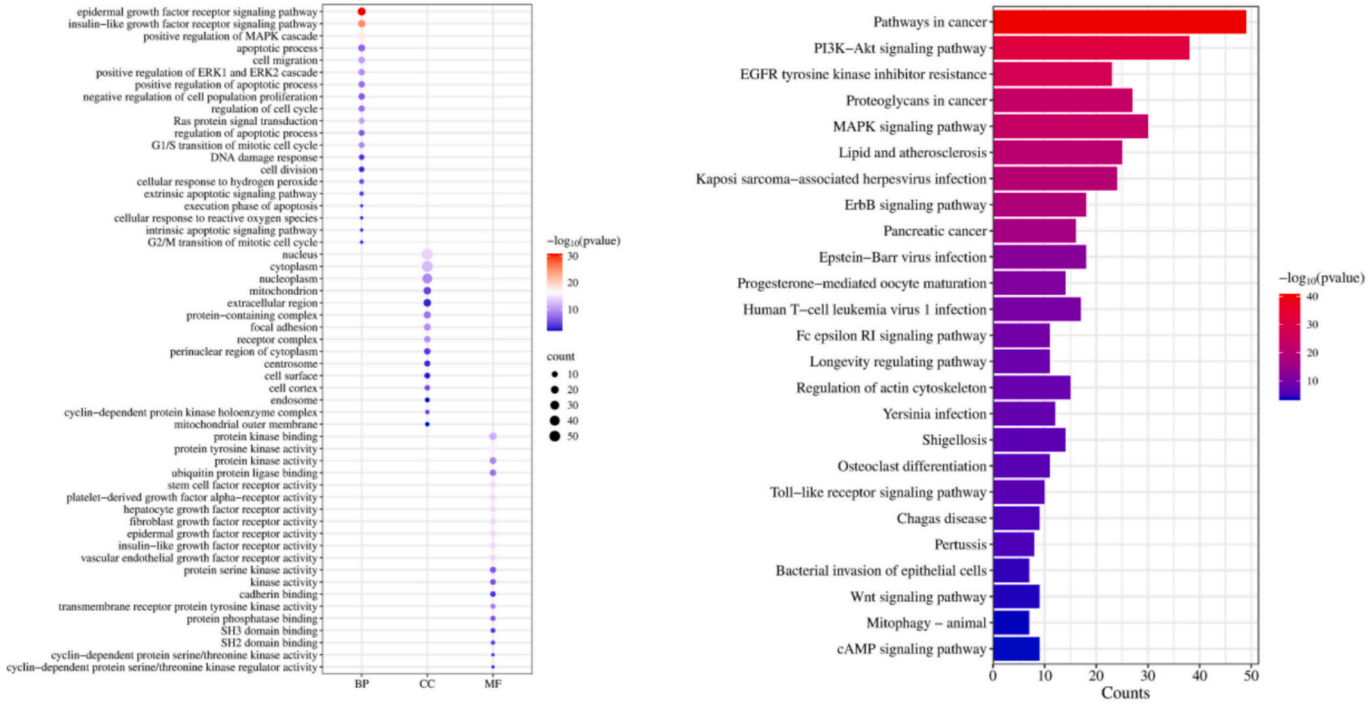

Fig. 4. GO Analysis (A) and KEGG Analysis (B).

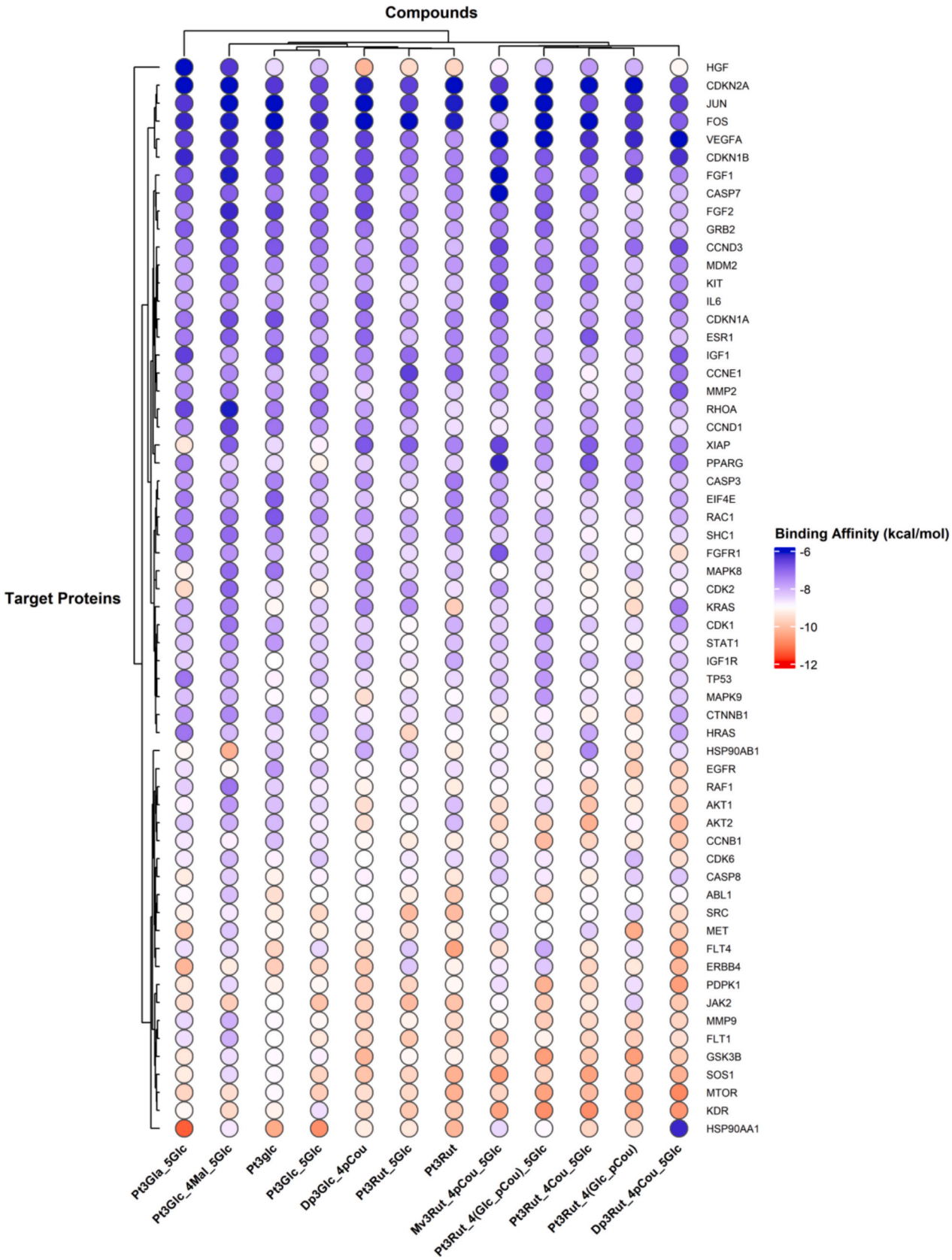

Fig. 5. Heatmap of the minimum binding energy from molecular docking.

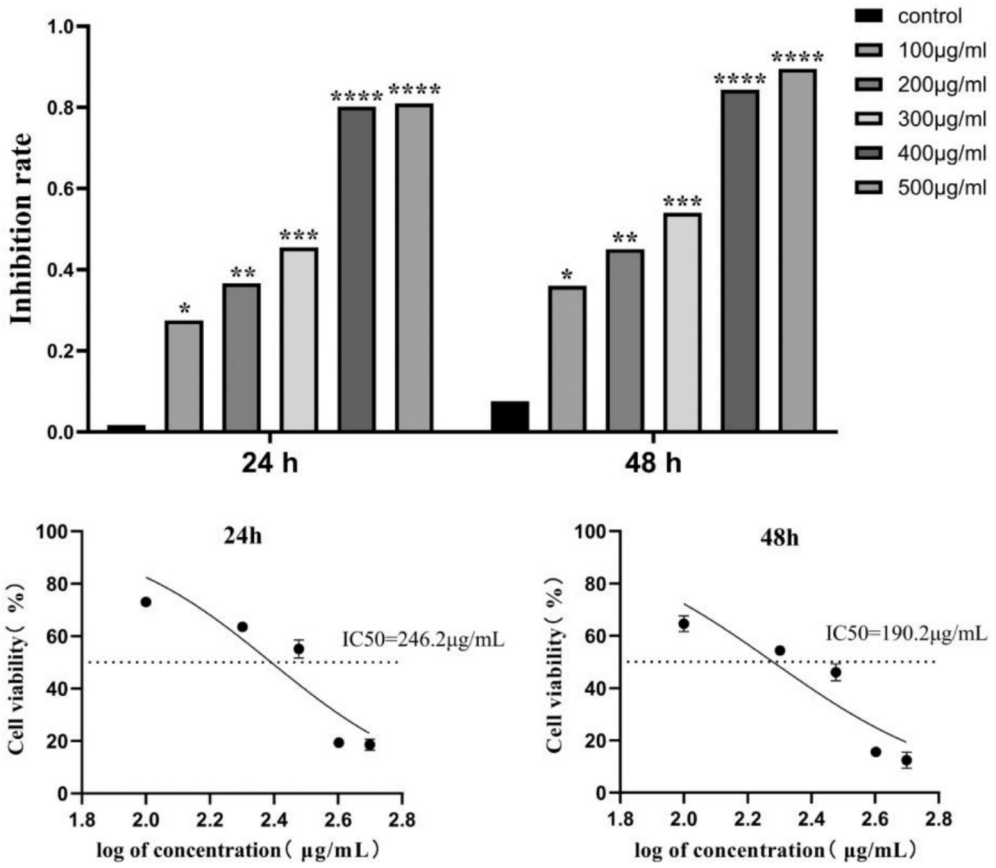

Fig. 6. Influence of varying concentrations of LRA on the rate of U251 cell proliferation inhibition after 24 and 48 hours.

with the species of Homo sapiens selected and the minimum relevance threshold set to 0.4. The data was then loaded into Cytoscape and subsequently analyzed using Centiscape 2.2 plugin to produce a protein-protein interaction (PPI) system using topological examination. Fig. 2 illustrates the PPI network of LRAs acting on GBM, displaying only the top 60 ranked targets. In this figure, red indicates core targets (degree $\geq$ 58), orange represents key targets (degree $\geq$ 41), and green signifies important targets (degree $\geq$ 20). The core targets highlighted in red revealed two critically significant pathways: RAS-MAPK (Motta et al., 2019) and PI3 K-AKT-mTOR (Peng et al., 2022).wo critically important pathways: RAS-MAPK (Motta et al., 2019) and PI3K-AKT-mTOR (Peng et al., 2022).

3.3. Gene enrichment analysis

The investigation performed ssGSEA overrepresentation analysis using the transcriptome data of normally cultured U251-MG cell lines, screening the top 10 enriched pathways for analysis and visualization (Fig. 3) to elucidate the initial characteristics of the U251 cell line. Subsequently, 66 functional targets associated with LRAs and GBM were input into the DAVID repository via GO molecular enhancement and KEGG pathway analysis. GO cellular augmentation yielded BP entries primarily involving EGFR signaling pathways, IGFBMP signaling pathways, positive regulation of MAPK cascades, apoptosis processes, cell migration, cell cycle regulation, and cellular responses to ROS. The Cellular Component (CC) entries predominantly pertained to nuclear, cytoplasmic, nucleoplasmic, mitochondrial, and focal adhesion components. The Molecular Function (MF) entries, totaling 138, were primarily associated with protein kinase interactions, including function of protein tyrosine kinases, function of protein kinases, ubiquitin-protein ligase binding, and activity of stem cell factor receptor (Fig. 4A). The KEGG pathway augmentation examination revealed a significant involvement of cancer-related signaling pathways, notably PI3K-Akt, MAPK, and EGFR, as depicted in Fig. 4B.

Using the ssgsea function to perform single-sample GSEA analysis revealed that, under normal culture conditions, the top ten enriched pathways in the U251-MG cell line were: Jak_STAT, Wnt_Signaling, TNF_Signaling, VEGF_Signaling, Cell_Cycle:, Apoptosis, Signaling pathways: MAPK and P53, mTOR_Signaling, PI3K_Akt.

Fig. 4A indicates that LRAs primarily exert their inhibitory effect on GBM U251 cells through various pathways, including EGFR, IGF-1R, MAPK, apoptosis regulation, cell cycle modulation, G1/S transition, and G2/M transition. Fig. 4B indicates that LRAs primarily exert their inhibitory effects on GBM U251 cells through signaling pathways including PI3K-Akt, EGFR, MAPK, p53, mTOR, TNF, JAK-STAT, Wnt, and cAMP.

3.4. Molecular docking and minimum binding energy analysis

In molecular docking, the top 60 core targets and 12 main LRA monomers were used. The structures of proteins were retrieved from PDB record, refined in Pymol to remove extraneous parts, and docked using AutoDock Vina. Negative binding energies indicated spontaneous binding, with lower values showing stronger affinity. All active LRA components exhibited binding energies below −5 kcal/mol, indicating favorable interactions with core targets (Fig. 5).

3.5. Effects of LRAs on the proliferative activity of human GBM U251 cells

The LRA-treated groups showed significantly different cell proliferation inhibition rates compared to the human GBM U251 reference group ($P < 0.05$). After 24 and 48 h under varying LRA concentrations, the proliferation inhibition rate of U251 cells significantly increased (*P*

Table 2
Comparison of proliferation inhibition rates (%) in U251 cells injected with distinct LRA concentrations at 24 and 48 h.

Group	24 h	48 h
Control	1.71	7.54
100 μg/mL	25.9 ①	32.9①
200 μg/mL	34.8①②	43.4①②
300 μg/mL	41.4①②③	51.4 ①②③
400 μg/mL	78.9①②③④	83.1①②③④
500 μg/mL	79.0 ①②③④⑤	89.7①②③④⑤

Note: ① Matched with the reference group, $P < 0.05$; ② Paralleled with the 100 μg/mL LRA group, $P < 0.05$; ③ Paralleled with the 200 μg/mL LRA group, $P < 0.05$; ④ Paralleled with the 300 μg/mL LRA group, $P < 0.05$; ⑤ Paralleled with the 400 μg/mL LRA group, $P < 0.05$.

< 0.05). Moreover, as drug concentration and exposure time increased, the cell proliferation inhibition rate exhibited a progressive upward trend, demonstrating clear dose-dependent and time-dependent effects (Fig. 6, Table 2). Since the three concentrations of 100, 300, and 500 μg/mL already exhibited a clear concentration-dependent trend in cell proliferation inhibition, and the results at 200 and 400 μg/mL were highly similar to those at the adjacent concentrations, subsequent experiments were performed using 0, 100, 300, and 500 μg/mL for mechanistic validation.

3.6. Impact of LRAs on human GBM U251 cell migration

Results from the cell scratch assay also validated that the therapy by LRAs significantly decreased U251 cell migration, and the effect was concentration-dependent (Fig. 7 and Fig. 8, Table 3). After 24 h, the migration rate of the control U251 cells was 29.5%, while that of cells treated with 500 μg/mL LRAs was significantly reduced to 4.2% ($P < 0.001$). Similarly, after 48 h, the movement level of the untreated U251 cells remained at 43.8%, while that of the cells treated with 500 μg/mL LRAs greatly decreased to 8.1% ($P < 0.001$). Furthermore, comparing migration rates across different concentration groups revealed that LRAs significantly inhibited U251 cell migration after 24 and 48 h ($P < 0.05$). This inhibitory effect markedly intensified with increasing LRA concentration and exhibited clear concentration- and time-dependent characteristics.

3.7. Impacts of LRAS on the cell cycle of human GBM U251 cells

The influence of LRAs on the cell cycle of human GBM U251 cells is shown in Fig. 9. Flow cytometry revealed a notable reduction in G0/G1 phase cell percentage with increased LRA concentrations, dropping from 84.58% in the control group to 73.18% in the 500 μg/mL group ($P < 0.01$).The G2/M phase cell proportion rose significantly from 6.49% in the control group to 9.81% in the 500 μg/mL group ($P < 0.01$), and the S-phase cell proportion also increased with higher LRA concentrations ($P < 0.01$). This indicates that LRAs may inhibit proliferation in human GBM U251 cells by causing a G2/M phase block and increasing the S-phase cell ratio. This phenotypic outcome aligns closely with preceding GSEA, GO, and KEGG enrichment analyses, collectively indicating that LRAs exert effects closely associated with routes comprising Cell Cycle, P53 Signaling, PI3 K-Akt Signaling, and MAPK Signaling.

3.8. Effects of LRAS on ROS levels in human GBM U251 cells

Relative to the control group, treatment with LRAs at different

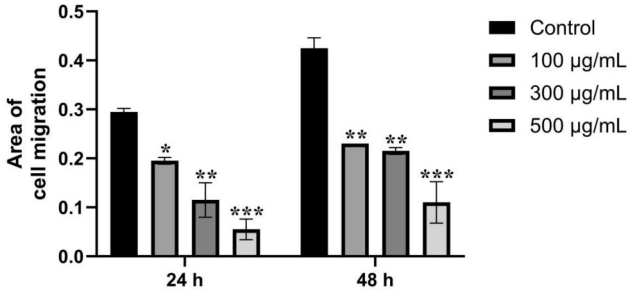

Fig. 8. Effect of different LRA concentrations on U251 cell migration rate at varying treatment durations.

Table 3
U251 cell migration rate as a function of LRA concentration and treatment duration (%).

Group	Control	100 μg/mL	300 μg/mL	500 μg/mL
24 h	29.5	19.6	9.5	4.2
48 h	43.8	23.3	20.7	8.1

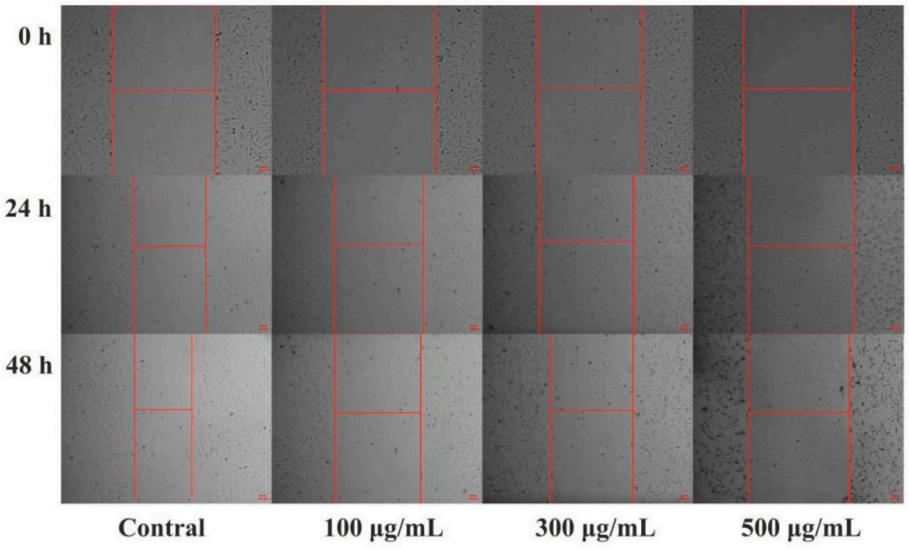

Fig. 7. Changes in cell migration of human GBM U251 cells at different LRA concentrations over varying exposure times (100× magnification).

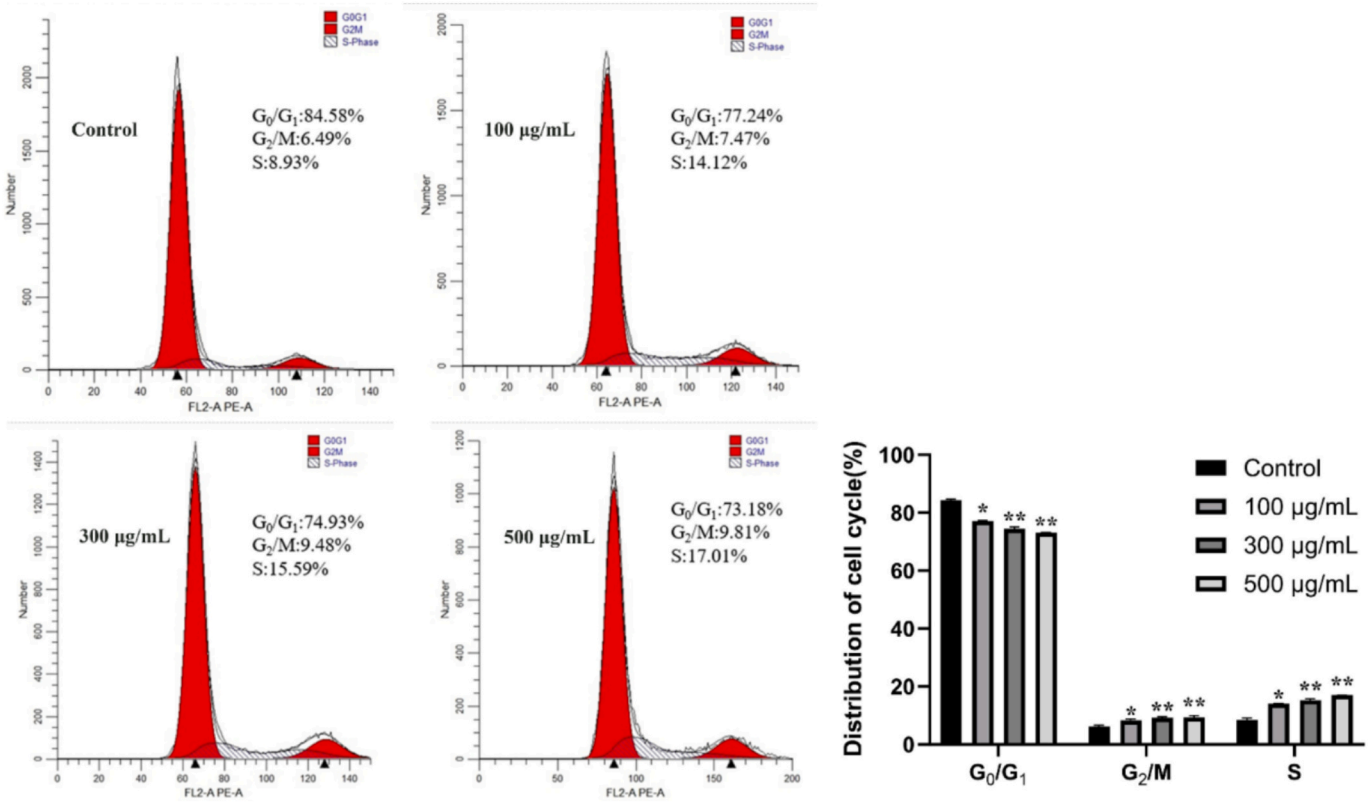

Fig. 9. Flow cytometry analysis of cell cycle spreading in humanGBM U251 cells exposed to different LRA concentrations for 24 hours.

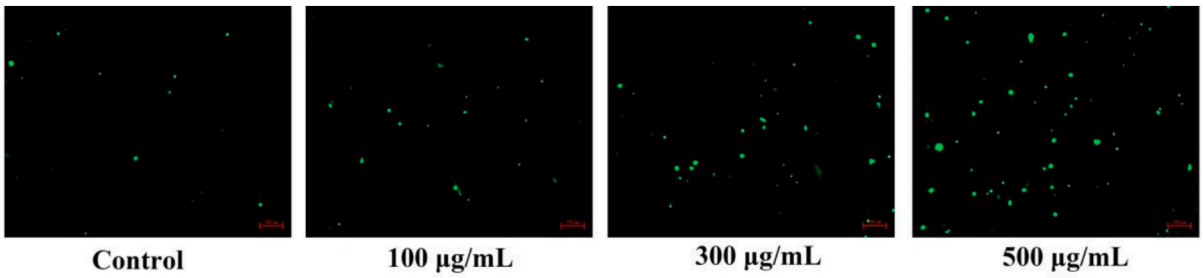

Fig. 10. Following a 24-hour treatment, the generation of ROS in human glioblastoma (GBM) U251 cells was measured with varying concentrations of latency-reversing agents (LRA), observed at 100× magnification.

concentrations led to a notable elevation in intracellular ROS levels in U251 cells. Moreover, this increase exhibited a concentration-dependent trend, progressively increasing with escalating LRA concentrations (Fig. 10). Previous studies have confirmed that elevated ROS levels can induce apoptosis by activating apoptotic signaling pathways. We therefore hypothesized that LRAs may promote apoptosis in human GBM U251 cells by inducing ROS production, thus activating ROS-mediated apoptotic signaling pathways.

3.9. Effects of LRAs on relative gene expression patterns of BAX, BCL-2, and CASPASE3 in U251 human GBM cells

The quantitative reverse transcription PCR (RT-qPCR) investigation showed that at both 24 h and 48 h post-treatment, compared to the sample, the magnitude of the BAX and CASPASE-3 mRNA levels of pro-apoptotic genes in human glioblastoma multiforme (GBM) U251 cells was significantly higher in response to the increasing concentrations of LRA (Figs. 11A, D and B, E). Conversely, BCL-2 mRNA levels significantly decreased (Fig. 11C, F) ($P < 0.05$). This alteration modulated the expression proportion of the apoptosis-associated molecular-level regulators *BAX* and *BCL-2*, thus promoting cell apoptosis. This result provides direct evidence, at the gene transcription level, for the pro-apoptotic effect of LRAs.

3.10. Effects of LRAs on the manifestation of proteins associated with apoptosis (Bcl-2, Bax, Caspase-3, Caspase-9, p53) in human GBM U251 cells

Western blot analysis showed that at both 24 h and 48 h post-treatment, LRAs led to a concentration-dependent reduction of *Bcl-2* and an escalation of *P53*, *Bax*, *Caspase-3*, and *Caspase-9* in comparison to the control group. These protein alterations were predicted by network pharmacology, molecular docking and qRT-PCR outcomes which were also characterized by the increased *BAX* and *CASPASE-3* mRNA and reduced *BCL-2* mRNA. Collectively, these findings associate gene expression and protein functions (Fig. 12).

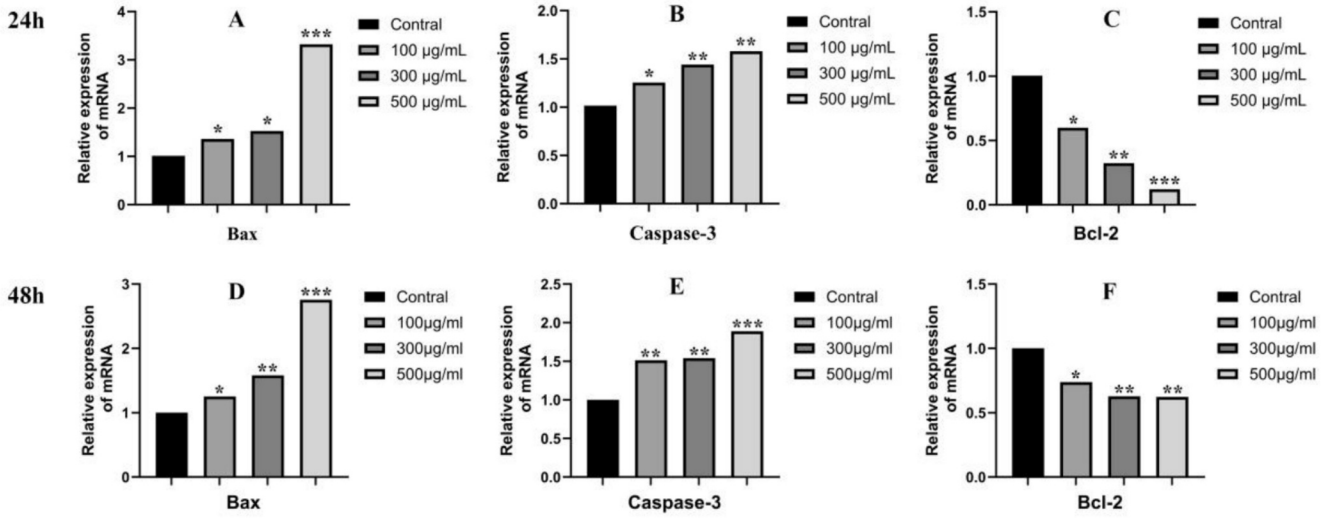

Fig. 11. RT-qPCR detection of gene expression levels in human GBM U251 cells across treatment groups at 24 h (A, B, C) and 48 h (D, E, F) post-treatment.

4. Discussion

GBM, as the predominant cancerous tumor of the CNS, exhibits clinical characteristics of high recurrence and mortality rates. Current clinical treatment regimens combining surgical resection with postoperative radiotherapy and chemotherapy can control disease progression to some extent. Nonetheless, the overall survival of the patients remains minimal (5-year postoperative survival rate < 20%), and the medication is excessively expensive and causes a heavy economic and healthcare burden to families and society (Wenlin et al., 2023). In recent years, the efficacy of combined Chinese and Western medicine on tumors has increasingly been apparent. This medicine relieves clinical symptoms and minimizes negative outcomes, including bone marrow suppression and gastrointestinal toxicity, induced by chemotherapy and radiotherapy; it also decreases tumor recurrences and improves patient survival, providing new hints on tumor treatments. Natural bioactive agents from Chinese herbal medicines have emerged as key materials for developing new anticancer medicines because they possess stable antitumor efficacy with low toxicity, high patient acceptability, and multitarget antitumor activity. For example, codonopsis pilosula glycosides (Liu et al., 2025), green tea catechin flavonoids (Zhan Sheng, 2020), and active ingredients, like *Tripterygium wilfordii* homofos (Du et al., 2025) and resveratrol (Wang et al., 2024), have been experimentally proven to display antitumor activity by suppressing tumor cells propagation and inducing apoptosis (Du et al., 2025). Active ingredients within resveratrol (Wang et al., 2024) have all been experimentally proven to display antitumor activity through mechanisms including the suppression of tumor cells' expansion and initiation of programmed cell death. *L. chinense* is a unique medicinal plant commonly found across northwestern China and other areas and is characterized by its fruits, rich in many anthocyanin components. It has been used in ethnic medical traditional settings for antioxidant and immune-enhancing purposes (Zeng et al., 2024). By combining network pharmacology and experimental justification, this study methodically explored the anti-GBM impacts and molecular mechanisms of LRAs, providing scientific backing for its traditional uses and medicinal potential.

Using a 'network pharmacology/in vitro cell/molecular docking tests' strategy, the study examined the anti-GBM mechanism of LRAs and identified 529 potential targets through network pharmacology screening.Intersecting these with 607 disease targets for GBM created 66 core-related targets. Network topology analysis of PPI networks further refined the latter to determine core functional targets. GO functional enrichment analysis subsequently revealed that the effect of the drug on disease targets primarily comprised biological processes involving apoptosis, cell migration, and cell cycle regulation. KEGG pathway enrichment analysis further revealed that LRAs acted on key pathways inside GBM U251 cells (i.e., PI3 K-Akt, EGFR, MAPK, and p53 activating trajectories). The binding of LRAs' active components to important target proteins was confirmed by molecular docking, suggesting a pharmacological basis for their anti-GBM action.

Based on these predictions, in vitro confirmation using human GBM U251 cells was obtained. MTT tests and wound-healing experiments proved that LRAs effectively inhibited U251 cell growth and migration in a concentration-dependent manner (Figs. 6 and 8), suggesting specific inhibition of GBM cell growth and invasion. Identification of ROS confirmed that ROS levels in U251 cells increased with LRA concentrations. ROS overproduction can cause intracellular biomolecules to be damaged through oxidative stress, ultimately leading to cell death. This discovery is concur with the prediction by network pharmacology on the enrichment outcome of "target mainly involved in apoptosis."

Apoptosis and cell cycle arrest are the ultimate biological processes that suppress tumor growth (Li et al., 2012). Programmed cell death is known as apoptosis, performs the key governing function for tumor initiation, progression, and therapeutic response (Mohammad et al., 2015). The network pharmacology analysis highlighted pathways linked to "apoptosis" and "cell cycle regulation," necessitating further validation of LRAs' effects on these processes in U251 cells. Flow cytometry showed that LRAs treatment decreased U251 cells in the phase of G0/G1 from 84.58% to 73.18%, while it raised G2/M phase's cells from 6.49% to 9.81% paralleled to the reference group. The outcome shows that LRAs are capable of stopping the U251 cell cycle at the G2/M stage, thus blocking injured cells from reaching mitosis and reducing tumor cell growth.Similarly, *Meng et al.*demonstrated that longikaurin A arrests U87 and SNB19 glioma cells (in the G2/M stage) via inhibiting the PI3K/AKT pathway, which supports the generality of G2/M phase arrest as an effective antiglioma strategy (Meng et al., 2023). RT-qPCR and western blot assessments additionally revealed that: (1) mRNA concentrations of the pro-apoptotic gene BAX and apoptotic mediator gene CASPASE-3 rose significantly, whereas the anti-apoptotic gene BCL-2 declined substantially; (2) at the protein level, anti-apoptotic protein Bcl-2 declined, whereas tumor suppressor protein P53, apoptosis-initiating enzyme caspase-9 and the pro-apoptotic protein Bax amplified. This result indicates that LRAs induce apoptosis in U251 cells by regulating the intrinsic apoptosis pathway (mitochondrial pathway). These conclusions aligns with Chen et al. (2022), who substantiated that grape seed proanthocyanidins downregulate Bcl-2 and upregulate P53 expression in C6 glioma cells, confirming the critical role of these key regulators in anthocyanin-mediated glioma cell apoptosis

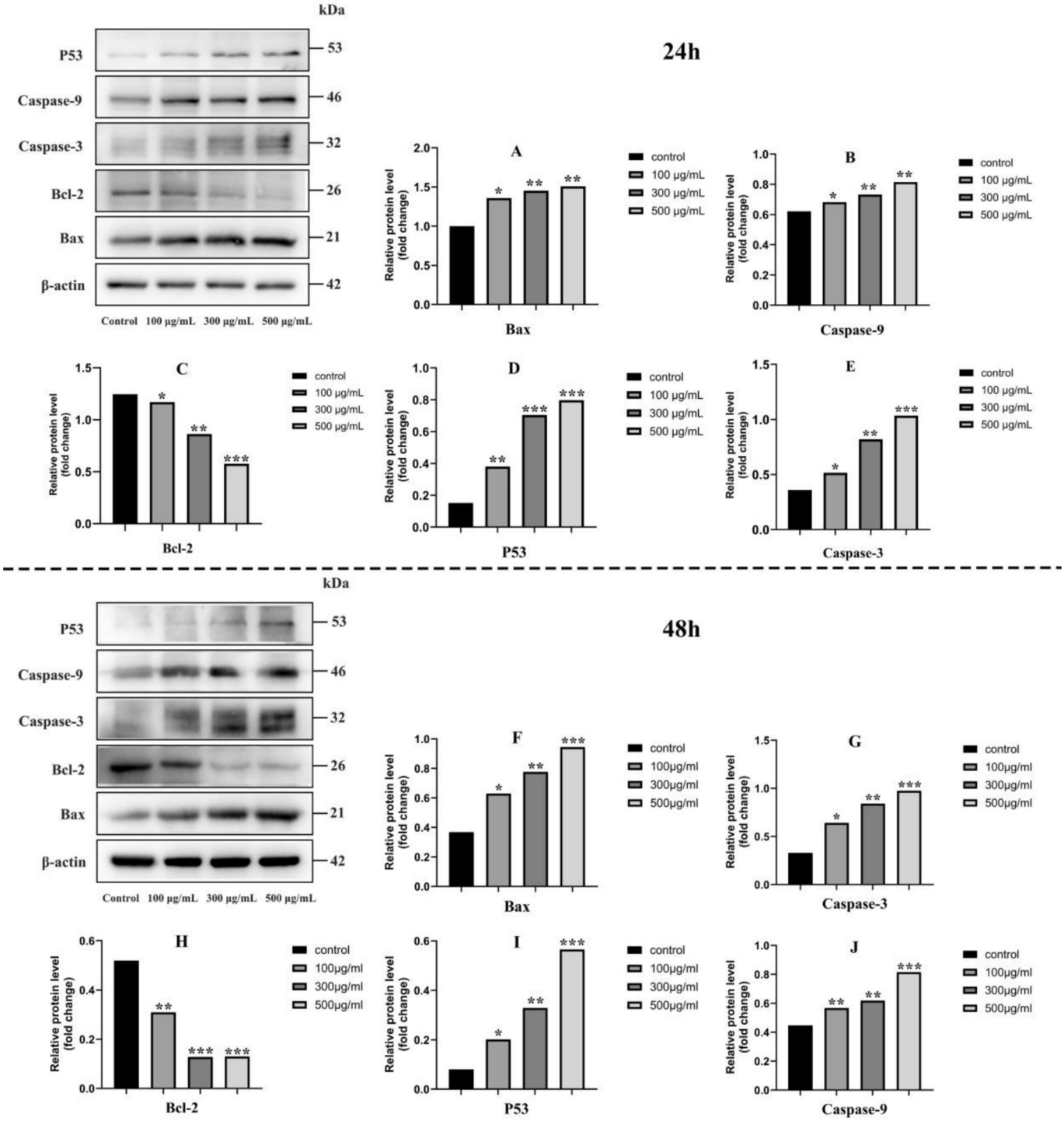

Fig. 12. Western blot detection of relevant protein expression levels in human GBM U251 cells across treatment groups at 24 h and 48 h post-treatment.

(Chen et al., 2022).

For tumor cells to survive, a key function is served by the PI3K-Akt pathway, with Akt as a key component. When phosphorylated, Akt inhibits caspase-9 and activates anti-apoptotic Bcl-2 proteins, preventing apoptosis in tumor cells (Cardone et al., 1998; Datta et al., 1997; Manning and Toker, 2017; Malak et al., 2025). Molecular docking results from this study indicate that LRAs can bind to Akt, while in vitro experiments demonstrated that Bcl-2's downregulation and caspase-9's upregulation, further confirming that LRAs can inhibit the PI3K-Akt pathway activity (reducing Akt phosphorylation levels), thus releasing the pathway's suppression of apoptotic signals and activating endogenous apoptotic pathways. It is important to note, however, that extensive crosstalk exists between the PI3K-AKT and MAPK pathways in glioma cells, where inhibition of one pathway can often lead to compensatory activation of the other, thereby affecting the overall therapeutic response(Fung et al., 2019). While our results confirm that LRAs effectively suppress PI3K-AKT signaling, their potential impact on the MAPK pathway—and the regulatory interplay between these two cascades—warrants further investigation to fully elucidate the anti-glioma mechanism of LRAs. In summary, LRAs combat GBM by binding to targets like Akt,blocking the PI3K-Akt pathway, increasing ROS levels, and halting the cycle of cell depicted in the G2/M stage, which

inhibits cell multiplication. By changing the Bax/Bcl-2 balance and activating the Caspase-9/Caspase-3 pathway, they induce cell death, which inhibits the proliferation and movement of U251 cells. These findings support recent studies showing that natural compounds like crebanine, pelargonidin, and mangiferin inhibit glioma through PI3K-Akt pathway suppression and mitochondrial apoptosis, highlighting this pathway as a key target for antiglioma natural products (Yeh et al., 2024; Tian et al., 2022).

5. Conclusion

Using network pharmacology and experimental validation, the study demonstrates that LRAs inhibit cell proliferation and migration, delay the stage of G_2/M by inducing production of ROS,and downregulate the signaling pathway of PI3K-Akt initiate the intrinsic apoptosis pathway (Bax/Bcl-2-Caspase-9/3), resulting in the destruction of U251 cells and indicating anti-GBM activity. These findings not only provide scientific support for the translational potential of LRAs as a natural-derived anti-GBM agent but also lay a theoretical foundation for developing novel GBM therapeutics based on this plant-derived anthocyanin-rich fraction.

CRediT authorship contribution statement

Hongwei Zhou: Writing – review & editing, Writing – original draft, Visualization, Resources, Funding acquisition, Formal analysis, Data curation, Conceptualization. **Jinwen Sima:** Writing – review & editing, Writing – original draft, Software, Resources, Formal analysis, Data curation, Conceptualization. **Shenglei Wang:** Writing – review & editing, Writing – original draft, Formal analysis, Data curation, Conceptualization. **Shijia Lu:** Writing – original draft, Formal analysis, Data curation, Conceptualization. **Jialin Liang:** Writing – original draft, Funding acquisition, Formal analysis, Data curation, Conceptualization. **Xinyao Li:** Writing – original draft, Formal analysis, Data curation, Conceptualization. **Tiantian Lian:** Writing – original draft, Formal analysis, Data curation, Conceptualization. **Congcong Wang:** Writing – original draft, Formal analysis, Data curation, Conceptualization.

Ethics Approval and Consent to Participate

Not applicable.

Patient consent for publication

Not applicable.

Funding

This research was funded by the National Natural Science Foundation of China, grant number 82072802; the Backbone Teachers Program of North Henan Medical University, grant number SQ2023GGJS03; Key Scientific Research Project of Institutions of Higher Education in Henan Province, grant number 25A310027 and the Henan Provincial Innovation and Entrepreneurship Training Program(Grant No. S202513505014).

Declaration of competing interest

The authors declare that they have no known competing financial interests or personal relationships that could have appeared to influence the work reported in this paper.

Appendix A. Supplementary data

Supplementary data to this article can be found online at https://doi.org/10.1016/j.gene.2026.150277.

Data availability

No data was used for the research described in the article.

References

Arrieta, V.A., Gould, A., Kim, K.S., Habashy, K.J., Dmello, C., Vázquez-Cervantes, G.I., Palacín-Aliana, I., McManus, G., Amidei, C., Gomez, C., Dhiantravan, S., Chen, L., Zhang, D.Y., Saganty, R., Cholak, M.E., Pandey, S., McCord, M., McCortney, K., Castro, B., Ward, R., Muzzio, M., Bouchoux, G., Desseaux, C., Canney, M., Carpentier, A., Zhang, B., Miska, J.M., Lesniak, M.S., Horbinski, C.M., Lukas, R.V., Stupp, R., Lee-Chang, C., Sonabend, A.M., 2024. Ultrasound-mediated delivery of doxorubicin to the brain results in immune modulation and improved responses to PD-1 blockade in gliomas. Nat. Commun. 15, 4698. https://doi.org/10.1038/s41467-024-48326-w.

Barrett T, Wilhite SE, Ledoux P, Evangelista C, Kim IF, Tomashevsky M, Marshall KA, Phillippy KH, Sherman PM, Holko M, Yefanov A, Lee H, Zhang N, Robertson CL, Serova N, Davis S, Soboleva A. NCBI GEO: archive for functional genomics data sets–update. Nucleic Acids Res. 2013 Jan;41(Database issue):D991-5. doi: 10.1093/nar/gks1193. Epub 2012 Nov 27.

Buccheri, R., Rescifina, A., 2025. High-throughput, high-quality: benchmarking GNINA and AutoDock Vina for precision virtual screening workflow. Molecules 30, 3361. https://doi.org/10.3390/molecules30163361.

Burley, S.K., Bhikadiya, C., Bi, C., Bittrich, S., Chao, H., Chen, L., Craig, P.A., Crichlow, G. V., Dalenberg, K., Duarte, J.M., Dutta, S., Fayazi, M., Feng, Z., Flatt, J.W., Ganesan, S., Ghosh, S., Goodsell, D.S., Green, R.K., Guranovic, V., Henry, J., Hudson, B.P., Khokhriakov, I., Lawson, C.L., Liang, Y., Lowe, R., Peisach, E., Persikova, I., Piehl, D.W., Rose, Y., Sali, A., Segura, J., Sekharan, M., Shao, C., Vallat, B., Voigt;, M., Webb, B., Westbrook, J.D., Whetstone, S., Young, J.Y., Zalevsky, A., Zardecki, C., 2023. RCSB Protein Data Bank (RCSB.org): delivery of experimentally-determined PDB structures alongside one million computed structure models of proteins from artificial intelligence/machine learning. Nucleic Acids Res. 51, D488–D508. https://doi.org/10.1093/nar/gkac1077.

Buzzao, D., Steininger, L., Guala, D., Sonnhammer, E.L.L., 2024. The FunCoup Cytoscape App: multi-species network analysis and visualization. Bioinformatics 41, btae739. https://doi.org/10.1093/bioinformatics/btae739.

Cabuk, K.S., Karabulut, G.O., Fazil, K., Nacaroglu, S.A., Gunaydin, Z.K., Taskapili, M., 2021. 2D analysis of gold weight implantation surgery results in paralytic lagophthalmos. Beyoglu Eye J. 6, 200–205. https://doi.org/10.14744/bej.2021.95866.

Cardone, M.H., Roy, N., Stennicke, H.R., Salvesen, G.S., Franke, T.F., Stanbridge, E., Frisch, S., Reed, J.C., 1998. Regulation of cell death protease caspase-9 by phosphorylation. Science 282, 1318–1321. https://doi.org/10.1126/science.282.5392.1318.

Chen, H.S., Lu, A.Q., Liang, J., Jin, M., Wei, Y., Yu, X.Y., Shang, Y.W., Huang, M., Chen, T.L., 2022. Effects of grape seed proanthocyanidins on reactive oxygen species, mitochondrial depolarization and expressions of STAT3, Bcl - 2 and P53P21 in rat C6 glioma cells. Chin. J. Tradit. Chin. Med. Sci. Technol. 29, 32–35. https://doi.org/10.3969/j.issn.1005-7072.2022.01.010.

Daina, A., Michielin, O., Zoete, V., 2019. SwissTargetPrediction: updated data and new features for efficient prediction of protein targets of small molecules. Nucleic Acids Res. 47, W357–W364. https://doi.org/10.1093/nar/gkz382.

Datta, S.R., Dudek, H., Tao, X., Masters, S., Fu, H., Gotoh, Y., Greenberg, M.E., 1997. Akt phosphorylation of BAD couples survival signals to the cell-intrinsic death machinery. Cell 91, 231–241. https://doi.org/10.1016/s0092-8674(00)80405-5.

Davis, A.P., Wiegers, T.C., Sciaky, D., Barkalow, F., Strong, M., Wyatt, B., Wiegers, J., McMorran, R., Abrar, S., Mattingly, C.J., 2025. Comparative toxicogenomics database's 20th anniversary: update 2025. Nucleic Acids Res. 53, D1328–D1334. https://doi.org/10.1093/nar/gkae883.

Dennis Jr, G., Sherman, B.T., Hosack, D.A., Yang, J., Gao, W., Lane, H.C., Lempicki, R.A. D.A.V.I.D., 2003. Database for annotation, visualization, and integrated discovery. Genome Biol. 4 (5), P3.

Du, X.D., Fan, M.Y., Xu, L.Q., Zhao, P.Y., Du, Z.X., Liu, Z., Hou, J.L., Liu, X.H., Yang, L.P., 2025. Study on anti-glioma mechanism of celastrol based on network pharmacology and experimental verification. Chin. J. New Drugs Clin. Rem. 44, 213–220. https://doi.org/10.14109/j.cnki.xyylc.2025.03.09.

G. Duarte Ramos Matos, S. Pak, R.C. Rizzo, Descriptor-driven de novo design algorithms for DOCK6 using RDKit, J. Chem. Inf. Model. 63 (2023) 5803-5822. Doi: 10.1021/acs.jcim.3c01031.

Erkisa, M., Sariman, M., Geyik, O.G., Geyik, C., Stanojkovic, T., Ulukaya, E., 2022. Natural products as a promising therapeutic strategy to target cancer stem cells. Curr. Med. Chem. 29, 741–783. https://doi.org/10.2174/0929867328666210628131409.

Fakhoury, K.R., Ney, D.E., Ormond, D.R., Rusthoven, C.G., 2021. Immunotherapy and radiation for high-grade glioma: a narrative review. Transl Cancer Res. 10, 2537–2570. https://doi.org/10.21037/tcr-20-1933.

Fan, H., Ji, Y., Wang, Y., Liu, D., Wei, T., Cao, X., Yang, M., Bai, C., Wang, Z., 2022. Anthocyanins from Lycium ruthenicum Murray inhibit HepG2 cells growth, metastasis and promote apoptosis and G2/M phase cycle arrest by activating the AMPK/mTOR autophagy pathway. Evid. Based Complement. Alternat. Med. 2022, 9609596. https://doi.org/10.1155/2022/9609596.

Fung, N.H., Grima, C.A., Widodo, S.S., Kaye, A.H., Whitehead, C.A., Stylli, S.S., Mantamadiotis, T., 2019. Understanding and exploiting cell signalling convergence

nodes and pathway cross-talk in malignant brain cancer. Cell Signal 59, 1–8. https://doi.org/10.1016/j.cellsig.2019.01.011.
Gallo K, Goede A, Preissner R, Gohlke BO. SuperPred 3.0: drug classification and target prediction-a machine learning approach. Nucleic Acids Res. 2022 Jul 5;50(W1): W726-W731. doi: 10.1093/nar/gkac297.
Gao, M., Meng, X.J., Li, X., Fan, J.L., Huang, L.L., Du, Y., Gao, N., Chen, S.N., Lou, H.H., Li, B., 2023. Research progress of symptom cluster assessment tools in patients with glioma. Chin. Nurs. Res. 37, 645–649. https://doi.org/10.12102/j.issn.1009-6493.2023.04.015.
Ghouzlani, A., Kandoussi, S., Tall, M., Reddy, K.P., Rafii, S., Badou, A., 2021. Immune checkpoint inhibitors in human glioma microenvironment. Front. Immunol. 12, 679425. https://doi.org/10.3389/fimmu.2021.679425.
Hamed, G., Omar, H.M., Sarhan, A.M., Salah, H.E., 2022. Proviral integration of Moloney virus-2 (PIM-2) expression level as a prognostic marker in patients with acute myeloid leukemia. Int. J. Gen. Med. 15, 4247–4258. https://doi.org/10.2147/ijgm.S354092.
Hamosh, A., Scott, A.F., Amberger, J.S., Bocchini, C.A., McKusick, V.A., 2005. Online mendelian inheritance in man (OMIM), a knowledgebase of human genes and genetic disorders. Nucleic Acids Res. 33, D514–D517. https://doi.org/10.1093/nar/gki033.
He, Y., Lin, Z., Tan, S., 2022. Identification of prognosis-related gene features in low-grade glioma based on ssGSEA. Front Oncol. 14 (12), 1056623. https://doi.org/10.3389/fonc.2022.1056623.
Hu, Y.K., Ablat, A., Bai, X.L., Yin, X., Ma, C., Liao, X., 2025. Phenolamides from rootstocks of Lycium ruthenicum Murr by ligand fishing and their neuroprotective effects. J. Agric. Food Chem. 73, 8944–8958. https://doi.org/10.1021/acs.jafc.4c11099.
Keiser, M.J., Roth, B.L., Armbruster, B.N., Ernsberger, P., Irwin, J.J., Shoichet, B.K., 2007. Relating protein pharmacology by ligand chemistry. Nat. Biotechnol. 25, 197–206. https://doi.org/10.1038/nbt1284.
S. Kim, J. Chen, T. Cheng, A. Gindulyte, J. He, S. He, Q. Li, B.A. Shoemaker, P.A. Thiessen, B. Yu, L. Zaslavsky, J. Zhang, E.E. Bolton, PubChem 2023 update, Nucleic Acids Res. 51 (2023) D1373-d1380. Doi: 10.1093/nar/gkac956.
Li, T., Kon, N., Jiang, L., Tan, M., Ludwig, T., Zhao, Y., Baer, R., Gu, W., 2012. Tumor suppression in the absence of p53-mediated cell-cycle arrest, apoptosis, and senescence. Cell 149, 1269–1283. https://doi.org/10.1016/j.cell.2012.04.026.
Li, F., Li, H., Li, S., He, Z., 2024. A review of Lycium ruthenicum Murray: geographic distribution tracing, bioactive components, and functional properties. Heliyon 10, e39566. https://doi.org/10.1016/j.heliyon.2024.e39566.
Li, Z.L., Mi, J., Lu, L., Luo, Q., Liu, X., Yan, Y.M., Jin, B., Cao, Y.L., Zeng, X.X., Ran, L.W., 2021. The main anthocyanin monomer of Lycium ruthenicum Murray induces apoptosis through the ROS/PTEN/PI3K/Akt/caspase 3 signaling pathway in prostate cancer DU-145 cells. Food Funct. 12, 1818–1828. https://doi.org/10.1039/d0fo02382e.
Liang, J., Ga, Z., Wu, J., Wang, Y., Dongzhu, N., Qieyang, R., Li, P., Huaqian, S., 2025. Lycium ruthenicum Murray anthocyanins alleviate aging through SIRT1/P53 signaling pathway. Int. J. Mol. Sci. 26, 4510. https://doi.org/10.3390/ijms26104510.
Liu, G., Jiang, R., Xu, C., Zhou, J., Liu, F., He, Z., Liu, Z., 2018. Survival analysis for high-grade glioma patients who received comprehensive treatment. J. Cent. South Univ. 43, 388–393. https://doi.org/10.11817/j.issn.1672-7347.2018.04.008.
Liu, M., Zhang, Y., Liu, Y.D., Zhang, X.F., Qiao, J.X., Feng, X.S., Liu, X.P., 2025. Regulatory role and mechanism of lobetyolin in the proliferation and apoptosis of brain glioma cells. Chin. J. Geriatr. Heart Brain Vessel Dis. 27, 952–958.
Malak, M.N., Arafa, E.A., Abdel-Fattah, M.M., Khalaf, M.M., Arab, H.H., Hamzawy, M.A., 2025. Targeting EGFR/PI3K/AKT/mTOR and Bax/Bcl-2/caspase3 pathways with ivermectin mediates its anticancer effects against urethane-induced non-small cell lung cancer in BALB/c mice. Tissue Cell 95, 102873. https://doi.org/10.1016/j.tice.2025.102873.
Manning, B.D., Toker, A., 2017. AKT/PKB signaling: navigating the network. Cell 169, 381–405. https://doi.org/10.1016/j.cell.2017.04.001.
Meng, X.R., Gao, Y.S., Sun, G., 2023. Longikaurin A inhibits glioma proliferation through phosphatidylinositol 3-kinase/protein kinase B pathway. Chin. J. Neuromedicine 22, 480–488. https://doi.org/10.3760/cma.j.cn115354-20221229-00942.
Mohammad, R.M., Muqbil, I., Lowe, L., Yedjou, C., Hsu, H.Y., Lin, L.T., Siegelin, M.D., Fimognari, C., Kumar, N.B., Dou, Q.P., Yang, H., Samadi, A.K., Russo, G.L., Spagnuolo, C., Ray, S.K., Chakrabarti, M., Morre, J.D., Coley, H.M., Honoki, K., Fujii, H., Georgakilas, A.G., Amedei, A., Niccolai, E., Amin, A., Ashraf, S.S., Helferich, W.G., Yang, X., Boosani, C.S., Guha, G., Bhakta, D., Ciriolo, M.R., Aquilano, K., Chen, S., Mohammed, S.I., Keith, W.N., Bilsland, A., Halicka, D., Nowsheen, S., Azmi, A.S., 2015. Broad targeting of resistance to apoptosis in cancer. Semin. Cancer Biol. 35 (Suppl), S78–s103. https://doi.org/10.1016/j.semcancer.2015.03.001.
Motta, M., Fidan, M., Bellacchio, E., Pantaleoni, F., Schneider-Heieck, K., Coppola, S., Borck, G., Salviati, L., Zenker, M., Cirstea, I.C., Tartaglia, M., 2019. Dominant Noonan syndrome-causing LZTR1 mutations specifically affect the Kelch domain substrate-recognition surface and enhance RAS-MAPK signaling. Hum. Mol. Genet. 28, 1007–1022. https://doi.org/10.1093/hmg/ddy412.
O'Boyle, N.M., Banck, M., James, C.A., Morley, C., Vandermeersch, T., Hutchison, G.R., 2011. Open babel: an open chemical toolbox. J Cheminform. 7 (3), 33. https://doi.org/10.1186/1758-2946-3-33.
Peng, Y., Wang, Y., Zhou, C., Mei, W., Zeng, C., 2022. PI3K/Akt/mTOR pathway and its role in cancer therapeutics: are we making headway? Front. Oncol. 12, 819128. https://doi.org/10.3389/fonc.2022.819128.
Rappaport, N., Twik, M., Plaschkes, I., Nudel, R., Iny Stein, T., Levitt, J., Gershoni, M., Morrey, C.P., Safran, M., Lancet, D., 2017. MalaCards: an amalgamated human disease compendium with diverse clinical and genetic annotation and structured search. Nucleic Acids Res. 45 (D1), D877–D887. https://doi.org/10.1093/nar/gkw1012.
Rosignoli, S., Paiardini, A., 2022. Boosting the full potential of PyMOL with structural biology plugins. Biomolecules. 12 (12), 1764. https://doi.org/10.3390/biom12121764.
Stelzer, G., Rosen, N., Plaschkes, I., Zimmerman, S., Twik, M., Fishilevich, S., Stein, T.I., Nudel, R., Lieder, I., Mazor, Y., Kaplan, S., Dahary, D., Warshawsky, D., Guan-Golan, Y., Kohn, A., Rappaport, N., Safran, M., Lancet, D., 2016. The GeneCards suite: from gene data mining to disease genome sequence analyses. Curr Protoc Bioinform. 20 (54). https://doi.org/10.1002/cpbi.5, pp. 1.30.1-1.30.33.
D. Szklarczyk, R. Kirsch, M. Koutrouli, K. Nastou, F. Mehryary, R. Hachilif, A.L. Gable, T. Fang, N.T. Doncheva, S. Pyysalo, P. Bork, L.J. Jensen, C. von Mering, The STRING database in 2023: protein-protein association networks and functional enrichment analyses for any sequenced genome of interest, Nucleic Acids Res. 51 (2023) D638-d646. Doi: 10.1093/nar/gkac1000.
Tian, Z., Sun, C., Liu, J., 2022. Pelargonidin inhibits vascularization and metastasis of brain gliomas by blocking the PI3K/AKT/mTOR pathway. J. Biosci. 47, 64. https://doi.org/10.1007/s12038-022-00281-8.
Wang, H., Li, J., Tao, W., Zhang, X., Gao, X., Yong, J., Zhao, J., Zhang, L., Li, Y., Duan, J. A., 2018. Lycium ruthenicum studies: molecular biology, phytochemistry and pharmacology. Food Chem. 240, 759–766. https://doi.org/10.1016/j.foodchem.2017.08.026.
Wang, X., Shen, Y., Wang, S., Li, S., Zhang, W., Liu, X., Lai, L., Pei, J., Li, H., 2017. PharmMapper 2017 update: a web server for potential drug target identification with a comprehensive target pharmacophore database. Nucleic Acids Res. 45 (W1), W356–W360. https://doi.org/10.1093/nar/gkx374.
Wang, Y., Wu, Y.Q., Deng, R.Q., Jin, Y.J., 2024. Study on the effect of resveratrol on the malignant behavior of glioma cells based on JAK2/STAT3 signaling pathway. Chin. J. Gerontol. 44, 6045–6050. https://doi.org/10.3969/j.issn.1005-9202.2024.24.035.
Wenlin, C., Yuekun, W., Qianshu, L., Liguo, Y., Zhiyao, Z., Xin, Z., Le, G., Yaning, C., Yixuan, S., Xiaopeng, G., 2023. Annual research progress of glioma in China in 2022. Med. J. Peking Union Med. Coll. Hosp. 14, 983–990. https://doi.org/10.12290/xhyxzz.2023-0321.
Xie, Z., Luo, Y., Zhang, C., An, W., Zhou, J., Jin, C., Zhang, Y., Zhao, J., 2023. Integrated metabolome and transcriptome during fruit development reveal metabolic differences and molecular basis between Lycium barbarum and Lycium ruthenicum. Metabolites 13, 680. https://doi.org/10.3390/metabo13060680.
Yao, Z.J., Dong, J., Che, Y.J., Zhu, M.F., Wen, M., Wang, N.N., Wang, S., Lu, A.P., Cao, D. S., 2016. TargetNet: a web service for predicting potential drug-target interaction profiling via multi-target SAR models. J. Comput. Aided Mol. Des. 30, 413–424. https://doi.org/10.1007/s10822-016-9915-2.
Yeh, P.S., Liu, C.T., Yu, C.Y., Chang, Y.C., Lin, S.Y., Li, Y.C., Luan, Y.Z., Sung, W.W., 2024. Crebanine, an aporphine alkaloid, induces cancer cell apoptosis through PI3K-Akt pathway in glioblastoma multiforme. Front. Pharmacol. 15, 1419044. https://doi.org/10.3389/fphar.2024.1419044.
Zeng, S., Lin, S., Wang, Z., Zong, Y., Wang, Y., 2024. The health-promoting anthocyanin petanin in Lycium ruthenicum fruit: a promising natural colorant. Crit. Rev. Food Sci. Nutr. 64, 10484–10497. https://doi.org/10.1080/10408398.2023.2225192.
Zhan Sheng, Z., 2020. Anticancer effects of catechin flavonoid in human glioma cells are mediated via autophagy induction, cell cycle arrest, inhibition of cell migration and invasion and targeting MAPK/ERK signalling pathway. J. BUON 25, 1084–1090. https://doi.org/10.3389/fonc.2020.01084.
Zhou, Y., Zhang, Y., Zhao, D., Yu, X., Shen, X., Zhou, Y., Wang, S., Qiu, Y., Chen, Y., Zhu, F., 2024. TTD: therapeutic target database describing target druggability information. Nucleic Acids Res. 52 (D1), D1465–D1477. https://doi.org/10.1093/nar/gkad751.

Glossary

LRA: Lycium ruthenicum anthocyanins
GBM: glioblastoma
MTT: MTT assay
ROS: Reactive Oxygen Species
RT-PCR: Reverse Transcription-Polymerase Chain Reaction
WB: Western Blotting
PI3K–AKT: Phosphatidylinositol 3-Kinase–Protein Kinase B
Bax: Bcl-2-Associated X Protein
Bcl-2: B-Cell Lymphoma 2
Caspase-3: Cysteine Aspartate-Specific Protease 3
Caspase-9: Cysteine Aspartate-Specific Protease 9
P53: Tumor Protein P53